Recent experimental study of DD fusion in the potential well of a virtual cathode at nanosecond vacuum discharge

A V Oginov[1,2], Yu K Kurilenkov[1], I S Samoylov[1], K V Shpakov[1,2], V P Tarakanov[1], V E Ostashev[1], A A Rodionov[1,2] and V T Karpukhin[1]

[1] Joint Institute for High Temperatures of the Russian Academy of Sciences, Izhorskaya 13 Bldg 2, Moscow 125412, Russia
[2] Lebedev Physical Institute of the Russian Academy of Sciences, Leninsky Avenue 53, Moscow 119991, Russia

E-mail: oginov@lebedev.ru

Abstract. Processes of nuclear burning of various elements in the scheme of a compact inertial electrostatic confinement implemented on the basis of a nanosecond vacuum discharge (NVD) with low-energy hollow cathode were investigated experimentally earlier. This paper presents the results of a recent series of DD fusion experiments on the newly created experimental set-up NVD-2 combined with x-ray and neutron yield diagnostics. The voltage-current (V–A) characteristics of the discharge, and the regimes of generation of x-ray and DD neutrons realized experimentally are presented and discussed. The experimental results are compared with the results of particle-in-cell simulation of the nuclear DD fusion processes in NVD using electrodynamic code KARAT. Recent series of DD fusion experiments have reproducing in TOF scheme some basic features of DD neutrons yield observed earlier. Meanwhile, the analysis of V–A characteristics and anode erosion shows that efficiency of energy deposition at initial stage of discharge is still insufficient, and the ways to optimize the electrophysical processes at NVD-2 are clarified.

1. Introduction

Inertial electrostatic confinement (IEC) was the first approximation to solve the problem of controlled nuclear synthesis and related schemes for fusion devices have been studied both experimentally and theoretically more than 50 years (see [1–7] and references therein). Purely electrostatic systems and combinations of magnetic and electrostatic systems have been explored. IEC schemes rely on accelerating ions to a fusion relevant energy range 50–200 keV using electric fields. The accelerating fields can be provided by grids or virtual cathodes [1–3]. Either spherical or cylindrical grids with high transparency are used with dc or low-frequency electric fields. Although IECs have demonstrating significant neutron yields in a compact table-top size and rather inexpensive devices, the fusion reactions are from nonthermal ions and resulting efficiency $Q = E_{\text{fusion}}/E_{\text{input}}$ is rather low ($\sim 10^{-8}$ or even less). The underlying problem is that for nonthermal systems, the Coulomb scattering cross sections are larger than the fusion cross sections.

Oscillating plasmas were suggested theoretically as a possible fusion scheme [8, 9], where oscillating ion cloud referred to as the periodically oscillating plasma sphere (POPS) may undergo a self-similar collapse in a harmonic-oscillator potential formed by uniform electron background. Theoretical study have indicated that such a scheme is highly effective and may result in net fusion energy gain $Q > 1$ even for DD fuel [10]. The experimental studies have confirmed the existence of the oscillating plasma [11, 12]. The proper scaling of the oscillations with both the ion mass and the potential well depth has been observed. A critical advantage for a POPS based fusion device is its favorable fusion power density scaling, which increases with the inverse of the virtual cathode radius [12]. This attribute provides an economical development path for the POPS concept since each next generation device will be smaller than the previous one. However, for the oscillatory plasmas, some theoretical results indicate that there are absolute limits on the achievable compressions at spherical geometry for perfect space charge neutralization [13]. In contrast, for the steady-state plasmas with small POPS oscillations, space charge neutralization is possible even in the quasineutral limit [13].

Unfortunately, the experimental studies of oscillating plasma at spherical geometry were interrupted rather soon after the first successful demonstrating of POPS approach at LANL [2, 11, 12]. Meanwhile, the cylindrical POPS-type system should be mentioned in experiments at IEC-scheme based on miniature nanosecond vacuum discharge (NVD) with deuterated Pd-anode [14–17]. In these experiments it had been demonstrated the version of a cylindrical virtual cathode (VC), where deuterium nuclei can be accelerated to energies of tens of keV at correspondent to VC potential well (PW) [15, 17]. In particular, POPS-like oscillations of deuterons in potential well of virtual cathode (called as multiple fusion events in [14]) followed by pulsating neutron yield were recognized at early NVD experiments [14, 18, 19]. Such a discharge operation mode is a certain analogue of POPS-based IEC fusion [8, 12] that was confirmed by a detailed numerical particle-in-cell (PIC) modeling of experiments with NVD by KARAT code [15, 17]. Also, the coincidence of the measured frequency of neutron yield pulsation in NVD with the calculated value of ion oscillation POPS frequency [12] is take place [15]. Already at this stage in the experiments with NVD the potential wells of virtual cathode of tens of kilovolts, VC radius $r_{\rm vc} \sim 0.1$ cm, and the ion oscillation frequencies of about 80 MHz were implemented [14,15,17,20]. Note, these characteristics of IEC fusion cell are close to the features of related potential elements in a modular, high mass power density POPS-based IEC fusion device discussed in LANL earlier [12].

In fact, the physics of the collisional DD synthesis at small-scale low energy vacuum discharge with deuterium-loaded Pd anodes have been clarified definitely during last years [20–22]. However, strongly interdisciplinary character of nuclear burning at NVD needs further theoretical and more sophisticated experimental studying. Meanwhile, previous experimental work on hard x-rays and DD neutrons generation at NVD [14, 18, 19] have allowed to get data-base for further theoretical study and simulations [15, 17], but to present time the experimental work itself was interrupted. Thus, the anew creating experimental stand NVD-2 combined with x-rays and neutron yield diagnostics is under construction now. This paper presents some first results and discussion of the new experiments on DD fusion at IEC-scheme realized on the basis of nanosecond vacuum discharge at the new experimental stand, NVD-2.

2. Experimental set-up and diagnostics

The general scheme and view of new experimental set-up are given in figure 1. The source of complex plasma (figure 1) consists of a cylindrical vacuum chamber with a diameter of 50 mm, which has three windows covered by a 70 micron Mylar film. The chamber is connected to a vacuum pump (to 10^{-6} mbar) continuously operating during a series of discharges. Two electrodes are situated on one axis: a cylindrical anode with varied number of Pd tubes and a hollow Al cathode [21]. The effective distance between the electrodes varies with a step of

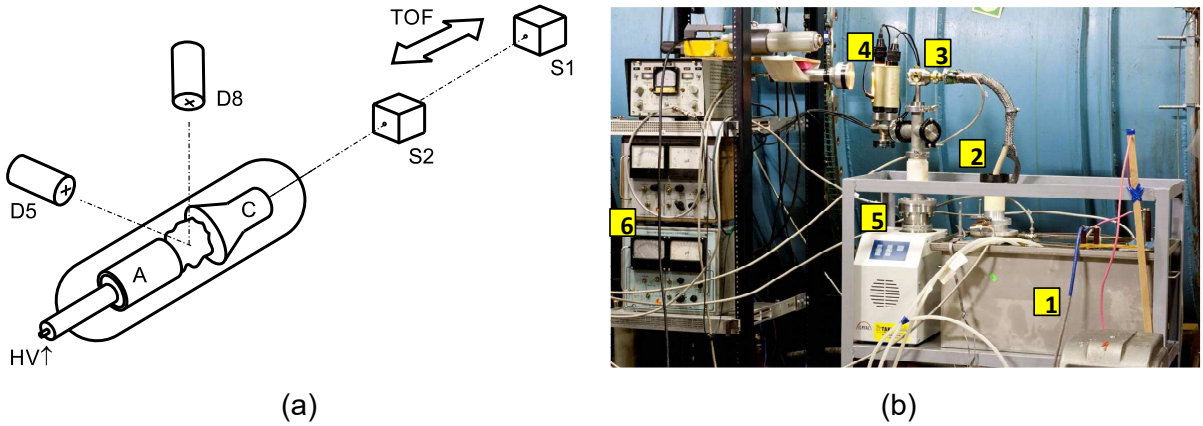

Figure 1. Schematic of the NVD-2 experimental setup (a): HV—high voltage pulse generator (HVPG) input, A— anode, C—cathode, S1 and S2—scintillation detectors for neutrons, D5 and D8—x-ray scintillation detectors, TOF— time-of-flight base. View of NVD-2 setup (b): 1—oil-filled HVPG, 2—high voltage output from the connector in an oil bath, 3—vacuum chamber with the anode assembly, 4—vacuum sensors, 5—vacuum station, 6—vacuum gauges.

0.1 mm in a range of few mm. The source includes a coaxial high voltage cable (with an impedance of 50 Ω) connected to the six-stage Marx generator sending a 70 ns pulse with a voltage up to 130 kV to a load of 50 Ohm. Commonly, the current comes up to 1.5 kA. Three Mylar windows provide for measuring x-rays in three perpendicular directions (in the plane approximately coinciding with the anode edge, figure 1a). Another window and/or time of flight (TOF) tube provide measuring through the edge of the hollow cathode (along cylindrical axis Z, figure 1a).

We investigated experimentally the generation of x-ray and neutron radiation in the NVD diode (figure 1) using a set of four "fast" radiation detectors based on two types of photomultipliers with high anode characteristics ($\sim$ 1 kA/lm), nanosecond time resolution, shielded against electromagnetic interference in the assembly with fast scintillators. In the development of the detector housings special attention is paid to the screening of the pulsed electromagnetic interference occurring at the time of discharge, for which elements of their design (multilayer shell of photomultiplier dynode system) were made of permalloy 79NM type.

X-rays with a resolution of 5 ns are recorded using detectors D5 and D8 (close to the chamber, see figure 1) based on FEU-85 type photomultipliers with fast x-ray scintillators (70 mm in diameter) and optimized dividers. Simultaneously with the measurement of x-ray yield, we work at this stage (as during the early experiments [14–16]) with deuterated palladium anodes and use TOF diagnostics of DD neutrons. For these purposes we are using a pair of S1 and S2 detectors with plastic scintillators (polystyrene with wavelength shifter 1.4-bis(5-phenyloxazol-2-yl) benzene, i.e. POPOP) of 150×50×55 mm^3 size located at different distances from the NVD chamber (figure 1). The ends of the scintillators via plexiglas light guides docked with the input windows of FEU-30 type photomultipliers. A scintillator + photomultiplier assembly with 5 cm thick lead shielding on all sides, except the edges (input windows of detectors) facing the radiation source. These windows closed by filters (Pb, Cu, Fe metal plate; borated polyethylene, etc.) of different thicknesses. The time resolution of the detector is determined by the decay of scintillators and is $\sim$ 10 ns (single pulse with a rise and fall at the level of 0.1). Electron transit times for different photomultipliers are vary in the range of 50–60 ns at a supply voltage of 2.0–2.2 kV for S1 and S2; and in the range of 25–40 ns at a supply voltage of 1.0–1.5 kV for D5 and D8. This fact, together with the geometry of detectors location, explains the time

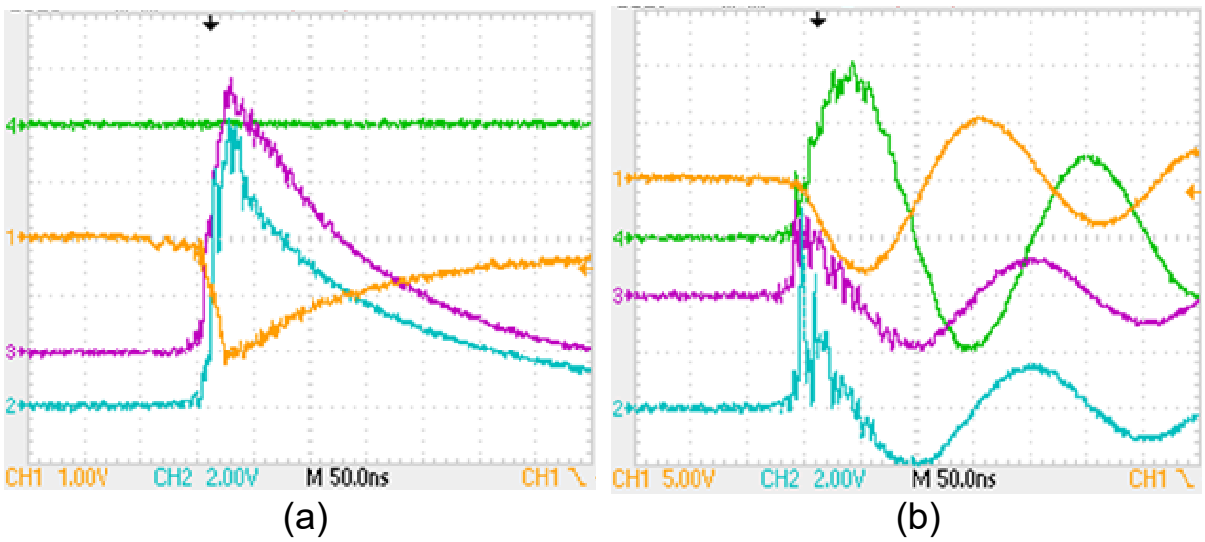

Figure 2. Calibration of electrophysical diagnostics: (a) idle mode and (b) the mode of "short circuit" (channels: 1—shunt of HVPG trigatron (1 V/div), 2—resistive divider (2 V/div); 3—capacitive divider; 4—reverse current shunt).

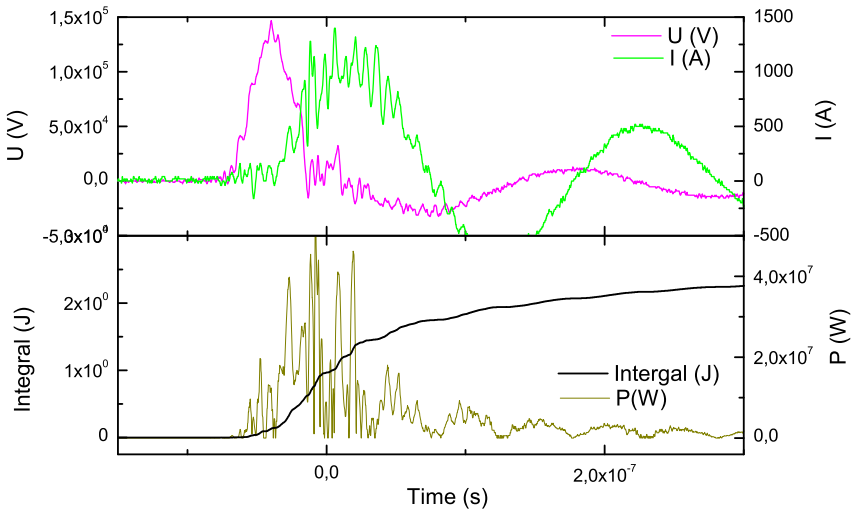

Figure 3. Volt-ampere (V–A) characteristics of discharge (top panel), total energy and power loaded (bottom panel).

shifts between traces 1.2 and 3.4 in figures 4a, 5a, 6a below. Data collected during a consecutive series of experiments, allow to draw conclusions about the energy spectra of the hard radiation, and their relationship with the characteristic features of current, voltage, power energy input behaviors during the initial phase of a nanosecond vacuum discharge. In addition, in figure 2 the calibration of electrophysical diagnostics is presented. With its use, for example, one can find the absolute value of the input voltage to the discharge chamber (channel 2 in figure 2). Sensitivity per single large cell on the channel 2 is equal to 2 V. Trace on channel 2 have about 10 V at the maximum, and since the conversion factor 12 [kV/V] (figure 2b), we have about 120 kV. Rather typical V–A characteristics as well as total energy and power loading are shown in figures 3–6 (their specifics are discussed below in section 4).

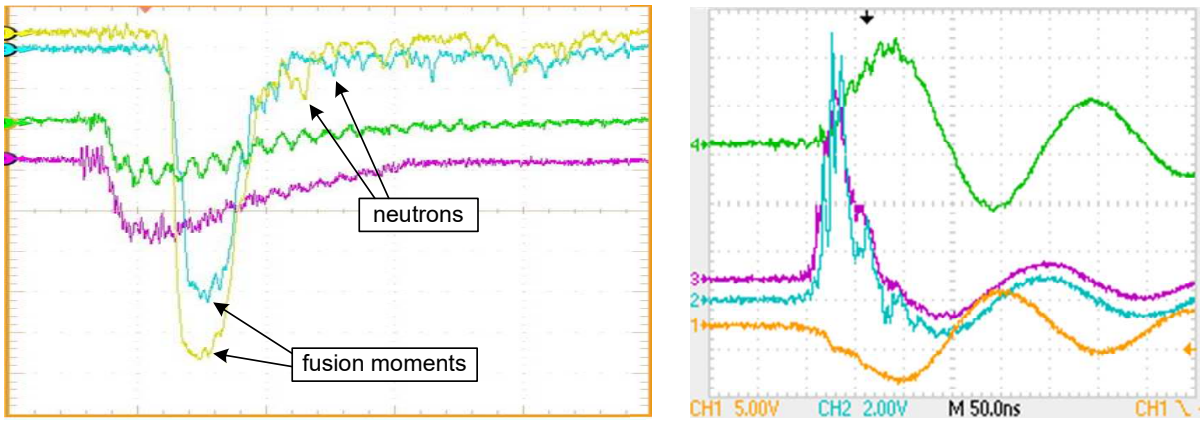

Figure 4. (a) Dynamics of x-ray and neutron yields in regime 1 and (b) V–A (blue-green) characteristics related in the same timescale (see caption in figure 2 and text for details).

3. Time-of-flight study of DD neutron yields

Neutron generation in interelectode space due to DD reactions of nuclear synthesis has been registered using a slightly simplified experimental set-up in comparison with previous x-ray and neutron yields studies [14–16]. The cylindrical Cu anodes (0.6 cm in diameter) have a set (3 or 12) of thin hollow deuterated Pd tubes (0.1 cm in diameter) attached to anode end-on, and the hollow cathode with conical part was performed from Al. The standard electrolysis in heavy water for about 6 hours at a current of 100 mA has been used for regular loading of Pd elements of the anode by deuterium. The principal scheme of the first measurements (figure 1a) corresponds to previous one [14–16]: along the axis anode-cathode the time-of-flight scheme for registration of DD neutrons through photomultipliers S1 and S2 (channels 1 and 2) with scintillators was arranged. X-ray yield in perpendicular direction have been registered by another type of photomultiplyes D5 and D8 (channels 3 and 4). The part of results obtained earlier have been reproduced now, and regimes were found experimentally when VC and correspondent PW were formed properly at interelectrode space. These regimes were accompanied by hard x-ray bursts and neutron yields. Examples of TOF study of DD neutron yield and correspondent V–A characteristics are given in figures 4–6.

In figure 4a traces of x-ray yields at perpendicular directions (channels 3 and 4) and x-rays and DD neutrons along the anode–cathode (A–C) axis (channels 1 and 2) for regime 1 are presented. V–A characteristics are shown in figure 4b. Photomultiplier S1 (yellow curve, channel 1) is located at 70 cm from source, and photomultiplier S2 (blue curve, channel 2)—at 120 cm from source. Remind, that the "signature" of coming of 2.45 MeV DD neutrons from reaction D + D $\rightarrow$ ^{3}He + n on photomultiplier S1 is delaying of signal for 46.6 ns/m.

The moments of synthesis (or extra x-rays due to bremsstrahlung of energetic products of synthesis—protons, tritium and ^{3}He) are shown near x-rays maxima in figure 4a (channels 1 and 2) by arrows. Note, spaced peaks on channel 1 and channel 2 are marked by arrows. First peak on yellow curve is delayed for about 33 ns from the moment of synthesis, meanwhile the difference in time between neutrons peaks is about 23 ns that corresponds to time-of-flight of DD neutrons between photomultipliers S1 and S2. More early in time some neutron peaks are overlapped and merged in the x-ray recession peak (channels 1 and 2). Meanwhile, channel 4 (green curve) represents well-defined oscillations with frequency $\sim$ 100 MHz. More or less similar traces for x-rays, DD neutrons and V–A characteristics for next shot (regime 2) are shown in figure 5.

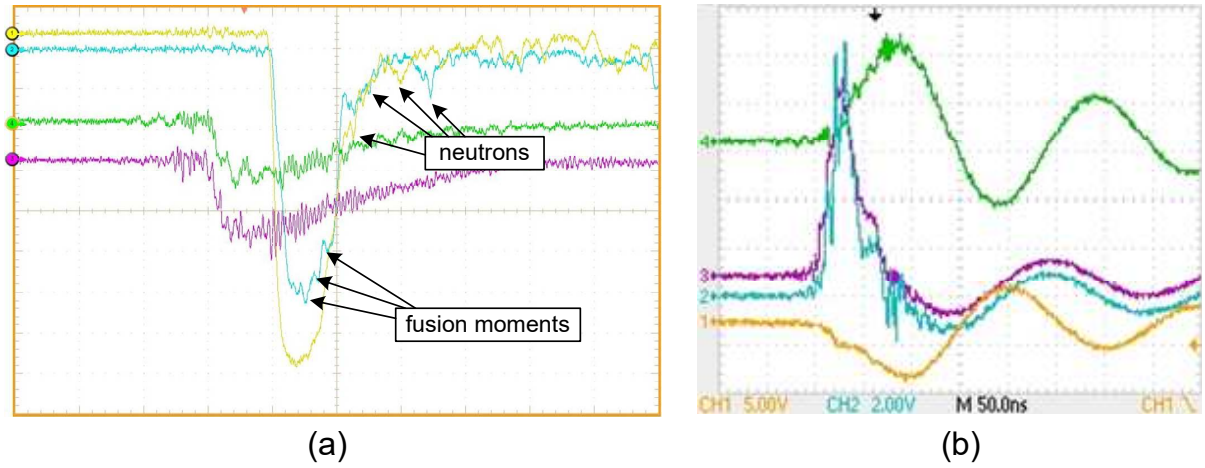

Figure 5. (a) Dynamics of x-ray and neutron yields in regime 2 and (b) V–A characteristics related.

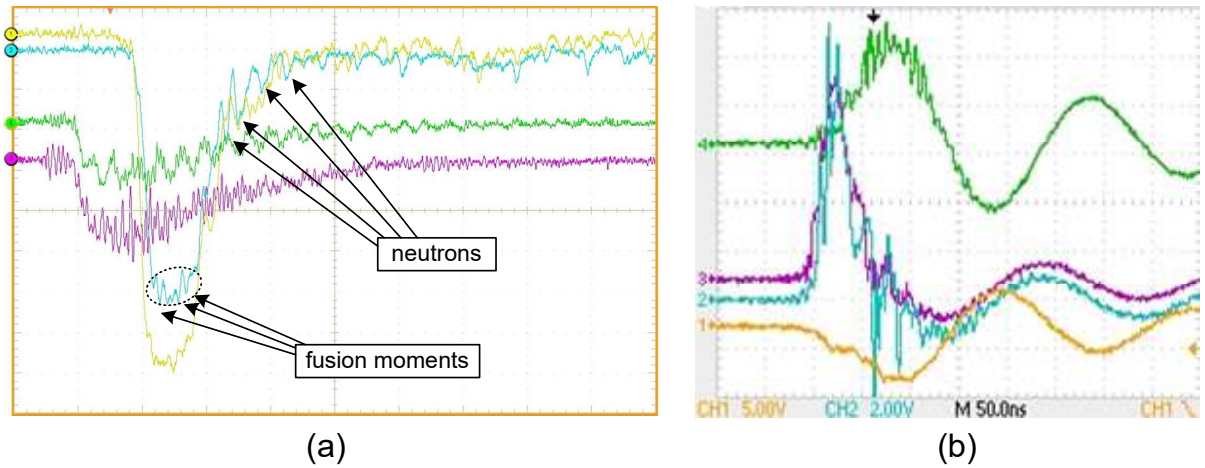

Figure 6. (a) Dynamics of x-ray and pulsating neutron yields in regime 3 and (b) related V–A characteristics.

Next shot (regime 3) with repetitive neutron yield which reminds pulsating neutron yields registered on previous experimental set-up [14–17] is presented in figure 6a. Four well-defined neutron peaks are observing in channel 2 (blue curve). Characteristic frequencies of deuterons oscillations in PW are about 60–70 MHz. Remark, as at previous experiments with NVD, this frequency is much higher than observed earlier under demonstration of POPS for non-deep PW at LANL [12].

4. PIC simulation with real V–A characteristics. Specifics of energy deposition.

The experimental work was accompanied by the particles-in-cell (PIC) simulation on the basis of electrodynamic code KARAT [23]. Note that at the initial stage of the experiment with NVD [14–16], we had a good voltage source with rather steep front (less than 5 ns). Earlier, the experimental data on particle dynamics and generation of the DD neutrons due to head-on collisions in a potential well of a virtual cathode were described properly by simulation in KARAT, where the almost constant voltage and current during the entire pulse was accepted [15, 17, 20]. With regard to the actual source (having higher output voltage and

twice the energy input), and volt-ampere characteristics listed above (figures 3, 4, 5a), the situation was different. We know, that the appearing of well-defined VC and correspondent PW is necessary to obtain the most interesting modes of x-ray and neutron generation [14, 20–22]. Meanwhile, PIC simulations of emergence of VC and PW with the loading of experimentally registered current-voltage characteristics (such as that shown in figures 4, 5) showing that a significant part of the total voltage pulse VC and PW are missing (poorly expressed VC and shallow PW), and appear in incomplete state just until the end of the pulse. Figure 7 is shown as an examples of the calculated VC (figure 7a,c) and PW (figure 7b,d) for simulation times 25 ns and 40 ns, respectively. We see from simulation that the VC at 25 ns is virtually nonexistent (figure 7a) and PW is poorly expressed and shallow (figure 7b), despite significantly larger voltage value at the pulse peak (120 kV) compared to the earlier experiment (70 kV) [14]. The same pattern is observed for 35 ns. In the area of 40 ns proper VC appears finally and the corresponding PW (figure 7d) becomes slightly deeper (maximum depth of about 50 kV). But on the 45th ns PW depth is again less than 30 kV, because the voltage already significantly drops although the current is still growing.

Analysis of the voltage and current characteristics and the erosion of the anode surface in various NVD modes showed a lack of efficiency of energy input to the initial phase of the discharge. Increasing of current reduces the voltage across the diode (figure 3, upper part). These features of the volt-ampere characteristics, arising from the strong feedback in the discharge circuit, cause rather late formation of VC and PW as well as consumption of part of the energy deposited for heating and melting the electrodes in an arc discharge stage. More preferable mode is the mode of voltage maintenance with an increase of current to a maximum and steeper voltage front. Therefore, at this stage of work the optimization paths of processes in electrical discharge through the forming line connecting diode and high voltage pulse generator (HVPG) are identified. In particular, it will provide conditions similar to TEM wave spreading in the diode gap, unlike the case of the direct pulse feeding of NVD chamber from HVPG. The proposed approach makes it possible to increase the lifetime of the potential well, to increase the output of the collisional DD synthesis without increasing the HVPG energy storage, to reduce the impact of the erosion of the anode Pd-tubes, to change the geometry of the diode parameters, to reduce the depletion of surface (working) layer of PdD_x anode.

Also, driving with an independent, galvanically isolated power supply will improve the signal/noise ratio of scintillation detectors. It eliminates the possibility of modulating the gain of photomultipliers at high pulse loadings possible in circuits with parallel high-voltage power supply. In general, it is possible to detect smaller flow of high-energy radiation, which is important for TOF measurements.

5. Concluding remarks

At the present new stage of experiment with NVD we have used old miniature discharge camera with the same periodically deuterated Pd anode and hollow cathode as in previous experiments, but with new power supply. Apparently, earlier in our steady-state plasmas in NVD device [14–16] (similar to one IEC considered theoretically in [4] for inverse polarity) the small POPS-like oscillations are primarily a mechanism to resonant heat the ions [13] rather than for coherent compressions as originally envisioned for POPS [8]. Also, our POPS-type NVD system with the deep potential well satisfies the stability conditions discussed in [4, 13] since ion temperature turns out comparable to the electron injection energy. Last but not least, electron injection in our discharge is going on from cathode surface to anode space from Pd tubes automatically when the voltage is applied (without special set of electron emitters like in [11, 12]), and observed deuterons oscillations turns out rather stable [14–16] (some other possibilities of realization of conditions for DD fusion under nanosecond laser influence were studied in experiments with convergent shock waves in conical targets [24]).

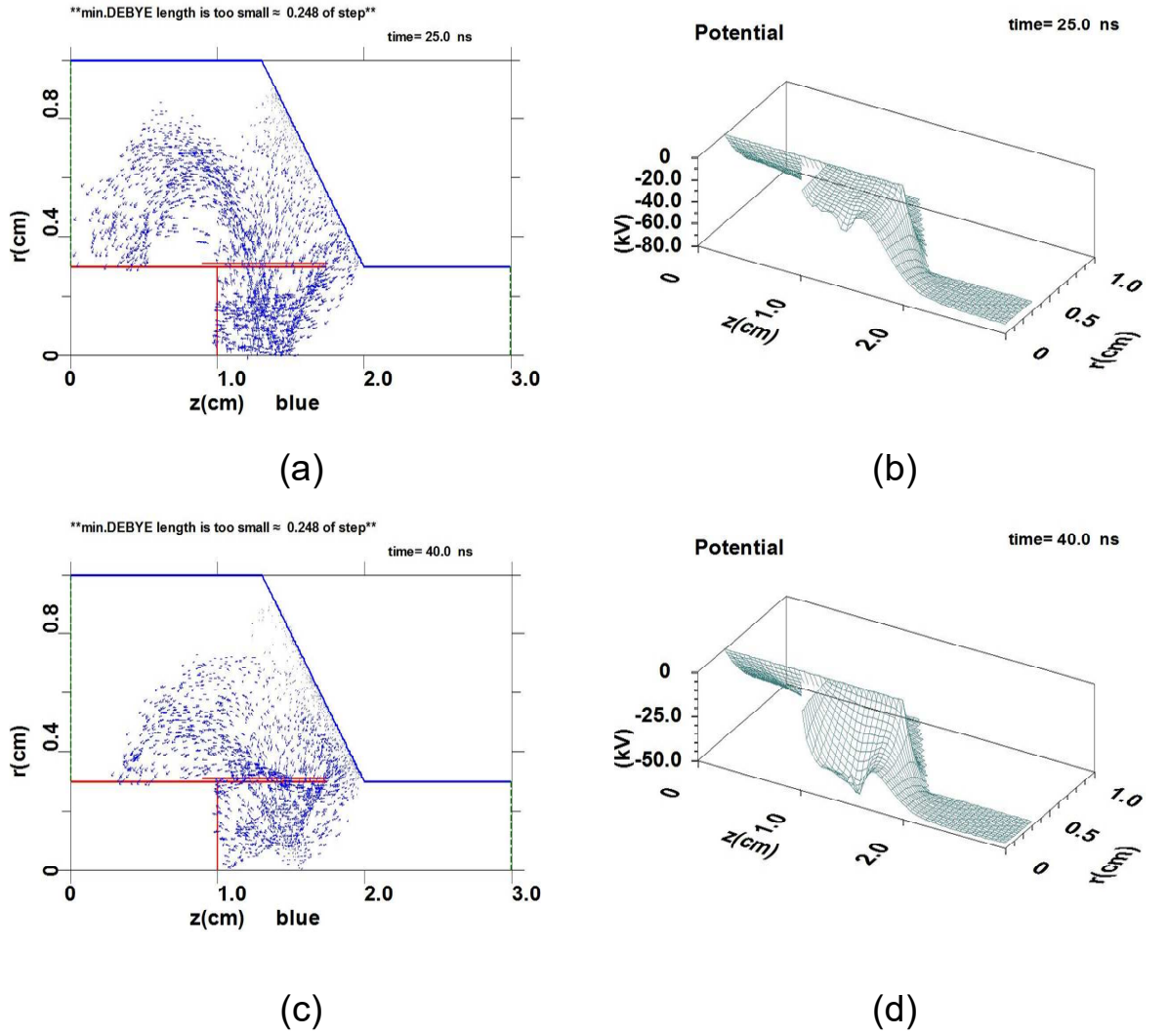

Figure 7. PIC simulation using KARAT code: (a) poorly defined virtual cathode at anode-cathode space (see [21]), and (b) narrow and non-deep potential well at 25th nanosecond; (c) proper virtual cathode at A–C space, and (d) more defined potential well at 40th nanosecond.

This paper represents an intermediate report related with construction of new experimental stand for studying the nuclear synthesis at the potential well of virtual cathode for ICF-scheme on the basis of NVD. At this stage of the work the stand NVD-2 is not fully completed by apparatuses for diagnostics of different processes, including x-ray spectral diagnostics. Nevertheless, the first TOF measurements are confirmed the DD neutron yield at ICF-scheme based on NVD. The total neutron yield is estimated as not less than $\sim 10^5/4\pi$ per shot. The part of previous features of DD fusion at NVD [14–16] is reproduced also, in particular, POPS-like multiple fusion events (figure 6a, channel 2). Meanwhile, PIC simulations with real V–A characteristics shows that rather limited and rather late neutron yield (like in figures 4a, 5a), probably, is the result of rather late formation of VC and correspondent PW (figure 7) during the voltage pulse applied from HVPG available now. From the other side, apparently, strong positive current fluctuations in regime 3 (figure 6b) would provide the appearance of noticeable and rather stable PW (earlier than in figure 7d) followed by deuterons oscillations and pulsating neutron yield related (figure 6a).

Note, we have used sometime in the experiments the different Pb filters (for channels 1, 2) to clarify better the neutron yield (on the background of x-rays) as well as we have changed A–C distances during searching the better conditions for proper formation of VC and PW, and, correspondingly, higher neutron yields. Also, data collected during a consecutive series of experiments, allow us to draw conclusions about the angular distributions of x-ray and neuron yields. This new data-base accumulating is the subject of further study and analysis also. Remark, the total energy deposition (figure 3) is higher than earlier [14, 18], but its going more slowly and with less efficiency for hard x-ray and neutrons generations since the essential part of energy deposited is just overheating the anode (some processes related have been studied in [25–27]). Thus, as noted above, our power supply should be optimized. Therefore, new HVPG and more efficient configurations of the anode-cathode (AC), with a good VC and deep PW has not been claimed yet in the present stage of experiments with NVD. Nevertheless, looking forward, we hope to use NVD-2 in the future for testing some theoretical predictions on achieving a positive energy yield of nuclear reaction and intense neutron generation [28], as well as to start the studying experimentally of the possibility of nuclear burning p + ^{11}B [22, 29] at potential well of virtual cathode in NVD.

Acknowledgments

The experimental study and simulations of DD fusion were supported by the Russian Science Foundation (grant No. 14-50-00124), the diagnostics of hard x-rays release is supported by the Russian Foundation for Basic Research (grant No. 15-08-0872).

References

[1] Lavrent'ev O A 2012 *On the History of Thermonuclear Synthesis in USSR* (Kharkov: Kharkov Phys.-Tech. Inst.) 2nd ed
[2] Miley G H and Murali S K 2014 *Inertial Electrostatic Confinement (IEC) Fusion* (New York: Springer)
[3] Dolan T J 1994 *Plasma Phys. Controlled Fusion* **36** 1539–1593
[4] Elmore W C, Tuck K M and Watson W C 1959 *Phys. Fluids* **2** 239–246
[5] Hirsch R L 1967 *J. Appl. Phys.* **38** 4522–4534
[6] Lavrent'ev O A 1975 *Ann. N. Y. Acad. Sci.* **251** 151–178
[7] Bussard R W 2006 *Proc. 57th Int. Astronaut. Congr. (IAC 2006)*
[8] Nebel R A and Barnes D C 1998 *Fusion Technol.* **38** 28–45
[9] Barnes D C and Nebel R A 1998 *Phys. Plasmas* **5** 2498–2503
[10] Chacon L, Miley G, Barnes D C and Krolll D A 2000 *Phys. Plasmas* **7** 4547–4560
[11] Park J, Nebel R A, Stange S and Murali S K 2005 *Phys. Rev. Lett.* **95** 015003
[12] Park J, Nebel R A, Stange S and Murali S K 2005 *Phys. Plasmas* **12** 056315
[13] Evstatiev E G, Nebel R A, Chacon L, Park J and Lapenta G 2007 *Phys. Plasmas* **14** 042701
[14] Kurilenkov Y K, Skowronek M and Dufty J 2006 *J. Phys. A: Math. Gen.* **39** 4375
[15] Kurilenkov Y K, Tarakanov V P, Skowronek M, Gus'kov S Y and Dufty J 2009 *J. Phys. A: Math. Theor.* **42** 214041
[16] Kurilenkov Y K and Skowronek M 2010 *Plasma Phys. Rep.* **36** 1219–1226
[17] Kurilenkov Y K, Tarakanov V P and Gus'kov S Y 2010 *Plasma Phys. Rep.* **36** 1227–1234
[18] Kurilenkov Y K, Skowronek M, Louvet G, Rukhadze A A and Dufty J 2000 *J. Phys. IV* **10** 409
[19] Kurilenkov Y K and Skowronek M 2003 *Pramana* **61** 1187–1196
[20] Kurilenkov Y K, Tarakanov V P, Gus'kov S Y, Karpukhin V T and Valyano V E 2011 *Contrib. Plasma Phys.* **51** 427–443
[21] Kurilenkov Y K, Tarakanov V P, Karpukhin V T, Gus'kov S Y and Oginov A V 2015 *J. Phys.: Conf. Ser.* **653** 012025
[22] Kurilenkov Y K, Tarakanov V P, Gus'kov S Y, Samoylov I S and Ostashev V E 2015 *J. Phys.: Conf. Ser.* **653** 012026
[23] Tarakanov V P 1992 *User's Manual for Code KARAT* (Va, USA: BRA Inc.)
[24] Krasyuk I K, Pashinin P P, Semenov A Y, Khishchenko K V and Fortov V E 2016 *Laser Phys.* **26** 094001
[25] Varaksin A Y and Zaichik L I 1998 *High Temp.* **36** 983–986
[26] Zaichik L I and Varaksin A Y 1999 *High Temp.* **37** 655–658
[27] Varaksin A Y 2016 *High Temp.* **54** 409–427

[28] Gus'kov S Y and Kurilenkov Y K 2016 Neutron yield and lawson criterion for plasma with inertial electrostatic confinement This issue
[29] Kurilenkov Y K, Tarakanov V P and Gus'kov S Y 2016 Simulation of proton–boron nuclear burning in the potential well of virtual cathode at nanosecond vacuum discharge This issue